*J. Fluid Mech.* (1978), *vol.* 87, *part* 4, *pp.* 761–771
*Printed in Great Britain*



# A note on the stability of a cylindrical vortex sheet

By RICHARD ROTUNNO

National Center for Atmospheric Research, Boulder, Colorado 80307

(Received 1 June 1977 and in revised form 3 January 1978)

An inconsistency in a previous stability analysis of a cylindrical vortex sheet is resolved. It is found that disturbances with azimuthal wavenumbers $m = 1$ and 2 are stable, whereas previously the stability of these modes was uncertain. It has been hypothesized that the multiple-vortex phenomenon is initiated by such an instability (Ward 1972). Since double vortices ($m = 2$) arise, we are led to consider a central downdraft surrounded by a uniform updraft; for a non-zero vertical wavenumber $\tilde{\gamma}$, the modes $m = 1$ and 2 are destabilized. Our theory is supported by the observation that double vortices tend to form as intertwining spirals (i.e. they have vertical structure).

## 1. Introduction

Michalke & Timme (1967) investigate the stability of a number of idealized flow fields pertaining to shear stability in cylindrical co-ordinates. The flow models are typically two or more concentric cylinders each of which is characterized by its mean circulation $\Gamma$. A certain inconsistency in their analysis has been resolved and is the subject of this article.

Consider the model consisting of two concentric cylinders; the inner cylinder is stagnant ($\Gamma = 0$) while the outer cylinder moves irrotationally ($\Gamma = \Gamma_0$, a constant). The two regions are separated by a cylindrical vortex sheet (i.e. since the vertical vorticity $\zeta = r^{-1}\partial\Gamma/\partial r$, the vorticity is everywhere zero except at the interface, where it is infinite). The result of the linear inviscid stability analysis of Michalke & Timme (1967) is that *all* azimuthal wavenumbers are unstable. Now consider the model consisting of three concentric cylinders; the inner and outermost cylinders have $\Gamma = 0$ and $\Gamma = \Gamma_0$, respectively. The cylinder between these two has $\Gamma = ar^2 + b$ (i.e. is a region of constant vorticity), where the constants are chosen such that the mean azimuthal velocity $V$ is continuous at the interfaces. Michalke & Timme (1967) and Busse (1968) find that all azimuthal wavenumbers $m$ *except* $m = 1$ and 2 are unstable. The inconsistency is that the characteristic equation for the model indicates that $m = 1$ and 2 are stable even in the limit of a vanishingly thin middle cylinder. Clearly, this limit is the model consisting of two concentric cylinders, the analysis of which indicates that *all* modes are unstable.

This problem has taken on new importance apart from its intrinsic academic interest. It has been hypothesized by Ward (1972) and Davies-Jones (1976) that multiple tornadic vortices are due to the instability of a cylindrical vortex sheet. Multiple vortices are observed in the laboratory (Ward 1972) as well as in nature (Fujita 1971). The author's interest in this problem was stimulated by Ward's (1972) experiment, where it is observed that the single vortex 'splits' into two vortices as a

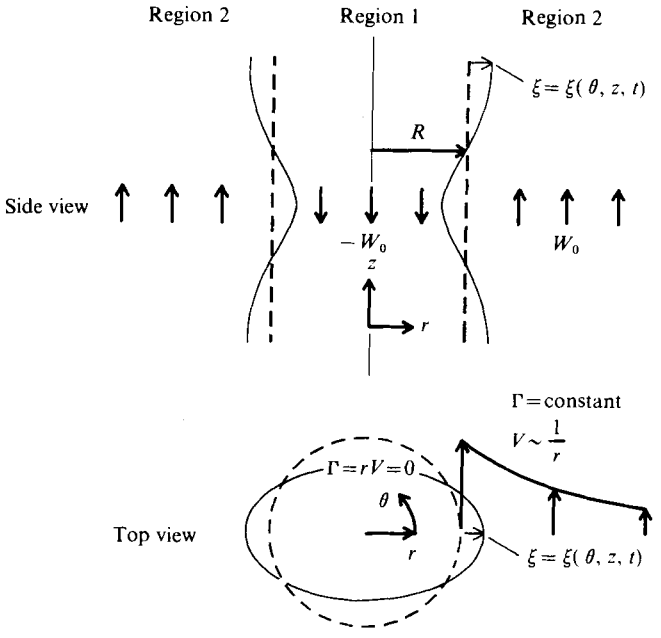


FIGURE 1. Schematic diagram of idealized flow whose stability is considered.

certain critical swirl ratio† is reached. Ward's hypothesis that these vortices are due to the instability of a cylindrical vortex sheet seems plausible. However, the stability analysis of Michalke & Timme (1967) leaves the question concerning the stability of $m = 1$ and 2 unanswered.

We have found that the model consisting of two concentric cylinders was treated incorrectly by Michalke & Timme (1967) and that modes $m = 1$ and 2 are *stable*. This implies that the multiple-vortex phenomenon is more complex than their simple shear-flow model would indicate.

At least two effects can destabilize these modes. Busse (1968) found that a skewed upper or lower surface destabilizes $m = 1$ and 2. Although there are no such skewed surfaces in Ward's model, we conjecture that the lower boundary layer may affect the flow stability. Another way in which these modes may become unstable is through the existence of substantial radial shear in the mean vertical velocity at the interface between the cylinders. Ward's experiment showed the existence of a central downdraft surrounded by an updraft. This effect can easily be incorporated in our analytical considerations and will be discussed later.

## 2. Derivation of the characteristic equation

Consider the flow in figure 1. There is an inner cylindrical region $0 \leqslant r \leqslant R$ containing a uniform downdraft $-W_0$ in which there is no azimuthal motion ($\Gamma = rV = 0$). The surrounding region $r > R$ has a uniform updraft $W_0$ and moves irrotationally ($\Gamma = \Gamma_0$, a constant). The vorticity is everywhere zero except at $r = R$, where it is infinite. That is, the vertical vorticity $\zeta = r^{-1}\partial\Gamma/\partial r$ and the azimuthal vorticity

† The swirl ratio is defined as $R\Gamma(R)/(2Q)$, where $R$ is the radius of the vortex chamber and $2\pi Q$ is the volume flow rate through the chamber.

$\eta = -\partial W/\partial r$ take on infinite values at $r = R$. We wish to study the stability of this flow with respect to small displacements $\xi$ of the material boundary separating the inner and outer regimes.

The flow in either region is irrotational, i.e. $\nabla \times \mathbf{u} = 0$, where $\mathbf{u}$ is the velocity vector in cylindrical co-ordinates. Thus $\mathbf{u} = \nabla\phi$, where $\phi$ is the velocity potential. In region 1

$$\phi = -W_0 z + \phi_1 \tag{2.1}$$

and in region 2

$$\phi = \Gamma_0\theta + W_0 z + \phi_2. \tag{2.2}$$

The independent variables $r$, $\theta$ and $z$ are defined in figure 1.

The equation describing the displacement of the vortex sheet is

$$r = R + \xi(\theta, z, t). \tag{2.3}$$

The vortex sheet acts as the outer boundary of the inner region, hence

$$\left(\frac{\partial\phi_1}{\partial r}\right)_{r=R+\xi} = \frac{D\xi}{Dt} = \frac{\partial\xi}{\partial t} + \frac{1}{r^2}\frac{\partial\phi_1}{\partial\theta}\frac{\partial\xi}{\partial\theta} + \left(-W_0 + \frac{\partial\phi_1}{\partial z}\right)\frac{\partial\xi}{\partial z}.$$

By assuming that products of perturbation variables are negligible, we obtain

$$\left(\frac{\partial\phi_1}{\partial r}\right)_{r=R} = \frac{\partial\xi}{\partial t} - W_0\frac{\partial\xi}{\partial z}. \tag{2.4}$$

Similarly, the vortex sheet acts as the inner boundary of the outer region. Thus

$$\left(\frac{\partial\phi_2}{\partial r}\right)_{r=R} = \frac{\partial\xi}{\partial t} + \frac{\Gamma_0}{R^2}\frac{\partial\xi}{\partial\theta} + W_0\frac{\partial\xi}{\partial z}. \tag{2.5}$$

Equations (2.4) and (2.5) are kinematical conditions. The dynamical condition which must be met is that the pressure be continuous across the interface, i.e.

$$(P_1 - P_2)_{r=R+\xi} = 0. \tag{2.6}$$

The pressure in an irrotational flow is (by Bernoulli's theorem)

$$P = \text{constant} - \rho(\partial\phi/\partial t + \tfrac{1}{2}[u^2 + v^2 + w^2]).$$

For the inner region,

$$P_1 = \text{constant} - \rho\left\{\frac{\partial\phi_1}{\partial t} + \frac{1}{2}\left[\left(\frac{\partial\phi_1}{\partial r}\right)^2 + \left(\frac{1}{r}\frac{\partial\phi_1}{\partial\theta}\right)^2 + \left(-W_0 + \frac{\partial\phi_1}{\partial z}\right)^2\right]\right\}. \tag{2.7}$$

Neglect of terms quadratic in the perturbation quantities leads to

$$P_1 = \text{constant} - \rho(\partial\phi_1/\partial t - W_0\,\partial\phi_1/\partial z). \tag{2.7a}$$

In the outer region,

$$P_2 = \text{constant} - \rho\left\{\frac{\partial\phi_2}{\partial t} + \frac{1}{2}\left[\left(\frac{\partial\phi_2}{\partial r}\right)^2 + \left(\frac{\Gamma_0}{R+\xi} + \frac{1}{R+\xi}\frac{\partial\phi_2}{\partial\theta}\right)^2 + \left(W_0 + \frac{\partial\phi_2}{\partial z}\right)^2\right]\right\},$$

or after linearization

$$P_2 \simeq \text{constant} - \rho\left(\frac{\partial\phi_2}{\partial t} + \frac{\Gamma_0}{R^2}\frac{\partial\phi_2}{\partial\theta} - \frac{\Gamma_0^2}{R^3}\xi + W_0\frac{\partial\phi_2}{\partial z}\right). \tag{2.8}$$

The third term in the brackets appears to have been omitted in the analysis of Michalke & Timme (1967). Leaving this term out of our analysis leads to the result that *all* azimuthal wavenumbers are unstable. The inclusion of this term yields a character-

istic equation in complete accord with the analyses for three concentric cylinders of both Michalke & Timme (1967) and Busse (1968). The dynamical condition is

$$\frac{\partial \phi_1}{\partial t} - \frac{\partial \phi_2}{\partial t} - W_0\left\{\frac{\partial \phi_1}{\partial z} + \frac{\partial \phi_2}{\partial z}\right\} - \frac{\Gamma_0}{R^2}\frac{\partial \phi_2}{\partial \theta} + \frac{\Gamma_0^2}{R^3}\xi = \text{constant}. \tag{2.9}$$

Equations (2.4), (2.5) and (2.9) form a linear system for three variables: $\xi$, $\phi_1$ and $\phi_2$. We solve this system for a particular Fourier component $e^{i(m\theta+\gamma z)}$ with the knowledge that any general disturbance can be described by an appropriate superposition of such components. The velocity potential $\phi$ satisfies Laplace's equation, i.e.

$$r^2\frac{\partial^2 \phi}{\partial r^2} + r\frac{\partial \phi}{\partial r} - (\gamma^2 r^2 + m^2)\phi = 0. \tag{2.10}$$

The general solution of (2.10) is

$$\phi = (B_1 I_m(\gamma r) + B_2 K_m(\gamma r))\, e^{i(m\theta+\gamma z)}, \tag{2.11}$$

where $B_1$ and $B_2$ depend on $t$ and $I_p(x)$ and $K_p(x)$ are modified Bessel functions of the first and second kinds, respectively. We require that $\phi$ be bounded both at the origin and infinity. Thus

$$\phi_1 = B_1 I_m(\gamma r)\, e^{i(m\theta+\gamma z)} \tag{2.12a}$$

and

$$\phi_2 = B_2 K_m(\gamma r)\, e^{i(m\theta+\gamma z)}. \tag{2.12b}$$

The solution for the displacement $\xi$ is of the form

$$\xi = D(t)\, e^{i(m\theta+\gamma z)}. \tag{2.13}$$

The next step is to substitute (2.12) and (2.13) into (2.4), (2.5) and (2.9). Note that the constant in (2.9) is set to zero since we are not concerned with solutions independent of $r$, $\theta$ and $z$. The result of this substitution is that

$$\{\gamma I_{m-1}(\gamma R) - mR^{-1} I_m(\gamma R)\} B_1 = \partial D/\partial t - i\gamma W_0 D, \tag{2.14}$$

$$\{-\gamma K_{m-1}(\gamma R) - mR^{-1} K_m(\gamma R)\} B_2 = \partial D/\partial t + (im\Gamma_0/R^2 + i\gamma W_0) D, \tag{2.15}$$

$$I_m(\gamma R)\frac{\partial B_1}{\partial t} - K_m(\gamma R)\frac{\partial B_2}{\partial t} - i\gamma W_0\{I_m(\gamma R) B_1 + K_m(\gamma R) B_2\} - \frac{im\Gamma_0}{R^2} K_m(\gamma R) B_2 + \frac{\Gamma_0^2}{R^3} D = 0. \tag{2.16}$$

$B_1$ and $B_2$ may be eliminated from (2.14)–(2.16) after some algebra. The result is

$$\frac{\partial^2 D}{\partial t^2} + \frac{2i}{\alpha+\beta}\left[(\beta-\alpha)\gamma W_0 + \beta m\frac{\Gamma_0}{R^2}\right]\frac{\partial D}{\partial t} + \left[-\gamma^2 W_0^2 - \frac{2\beta}{\alpha+\beta}\left(\frac{m\gamma\Gamma_0 W_0}{R^2}\right) - \frac{\beta}{\alpha+\beta}\frac{m^2\Gamma_0^2}{R^4} + \frac{\Gamma_0^2}{R^4}\frac{1}{\alpha+\beta}\right] D = 0, \tag{2.17}$$

where

$$\alpha \equiv \frac{I_m(\gamma R)}{\gamma R I_{m-1}(\gamma R) - m I_m(\gamma R)}, \quad \beta \equiv \frac{K_m(\gamma R)}{\gamma R K_{m-1}(\gamma R) + m K_m(\gamma R)}. \tag{2.18a, b}$$

We assume $D \sim e^{\sigma t}$ and define the non-dimensional quantities $\tilde{\sigma} \equiv \sigma R^2/\Gamma_0$, $\tilde{\gamma} = \gamma R$ and $S = W_0 R/\Gamma_0$. Equation (2.17) then becomes

$$\tilde{\sigma}^2 + \frac{2i}{\alpha+\beta}[\tilde{\gamma}(\beta-\alpha) S + \beta m]\tilde{\sigma} - \left[\tilde{\gamma}^2 S^2 + \frac{2\beta}{\alpha+\beta} m\tilde{\gamma} S + \frac{\beta m^2}{\alpha+\beta} - \frac{1}{\alpha+\beta}\right] = 0. \tag{2.19}$$

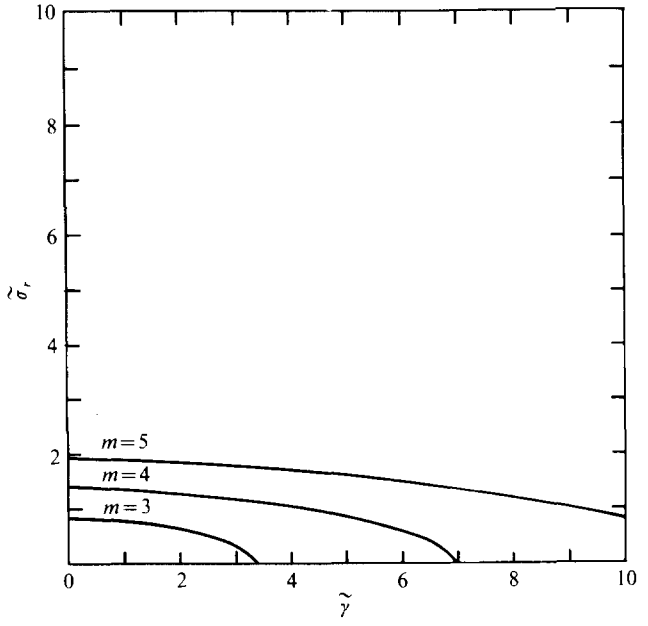


FIGURE 2. Non-dimensional growth rate $\tilde{\sigma}_r$ *vs.* the non-dimensional axial wavenumber $\tilde{\gamma}$ for azimuthal wavenumbers $m = 3, 4, 5$ derived from (3.1) ($S = 0$).

The solution is obtained from the quadratic formula, i.e.

$$\tilde{\sigma} = \frac{-i}{\alpha+\beta}[\tilde{\gamma}(\beta-\alpha)S+\beta m] \pm \left(\tilde{\gamma}^2S^2+\frac{2\beta}{\alpha+\beta}m\tilde{\gamma}S+\frac{\beta}{\alpha+\beta}m^2-\frac{1}{\alpha+\beta} - \frac{1}{(\alpha+\beta)^2}[\tilde{\gamma}(\beta-\alpha)S+\beta m]^2\right)^{\frac{1}{2}}. \tag{2.20}$$

If the quantity under the square root is positive, the particular configuration $(m, \tilde{\gamma})$ is unstable and grows exponentially with time. The following sections examine particular limiting cases of (2.20).

## 3. Case I: zero mean vertical velocity

Equation (2.20) becomes, after setting $S = W_0 R/\Gamma_0 = 0$,

$$\tilde{\sigma} = \frac{-i\beta m}{\alpha+\beta} \pm \left(\frac{\beta}{\alpha+\beta}m^2-\frac{1}{\alpha+\beta}-\frac{\beta^2m^2}{(\alpha+\beta)^2}\right)^{\frac{1}{2}}. \tag{3.1}$$

We consider the subcase where $\tilde{\gamma} \to 0$ so that direct comparison can be made with previous results. As $\tilde{\gamma} \to 0$, $\alpha = \beta \sim m^{-1}$. Hence

$$\tilde{\sigma} = -\tfrac{1}{2}im \pm \tfrac{1}{2}[m(m-2)]^{\frac{1}{2}}. \tag{3.2}$$

This result may be compared with equation (4.46) of Michalke & Timme (1967) (set $\tilde{\gamma} = 0$ and take the limit of $\beta_i$ as $\delta \to 1$) or with Busse's (1968) equation (5.7) (take the limit of this equation as $\tilde{\gamma} \to 1$). Thus, except for modes $m = 1$ and 2, the results of this analysis are analogous to those for the stability of a plane shear flow. There *all* wavelengths are unstable, the smallest waves growing most rapidly.

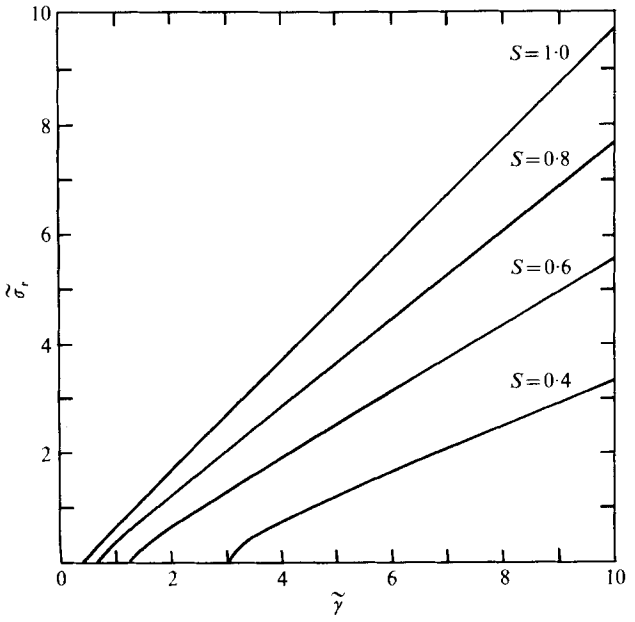


FIGURE 3. Non-dimensional growth rate $\tilde{\sigma}_r$ *vs.* the non-dimensional axial wavenumber $\tilde{\gamma}$ for $S = 0{\cdot}4$, $0{\cdot}6$, $0{\cdot}8$ and $1{\cdot}0$ derived from (4.1) ($m = 0$).

The real part of $\tilde{\sigma}$ is the non-dimensional growth rate $\tilde{\sigma}_r$. Figure 2 shows a graph of $\tilde{\sigma}_r$ *vs.* $\tilde{\gamma}$ [derived from (3.1)] for $m = 3, 4$ and 5. The modes $m = 1$ and 2 are stable for all $\tilde{\gamma}$. Figure 2 indicates that, for a given $m$, the most unstable wave is one which has no axial variation ($\tilde{\gamma} = 0$). Remember that $S = 0$ implies that there is no radial shear in the mean vertical velocity, and hence that the only way in which the disturbances may grow is by feeding upon the energy in the radial shear in the mean azimuthal velocity. For large $\tilde{\gamma}$, the wavenumber vector becomes nearly parallel to the mean flow vector and thus the wave is not as strongly affected by the mean flow. In the limit $\tilde{\gamma} \gg m \gg 1$, (3.1) becomes

$$\tilde{\sigma} \sim \pm i(\tfrac{1}{2}\tilde{\gamma})^{\frac{1}{2}}, \tag{3.3}$$

which demonstrates the stability of the disturbance in this limit.

## 4. Case II: axisymmetric disturbances, $m = 0$

Consider (2.20) with $m = 0$. Then

$$\tilde{\sigma} = -i\tilde{\gamma}S\left(\frac{\beta-\alpha}{\beta+\alpha}\right) \pm \left(\tilde{\gamma}^2S^2 - \tilde{\gamma}^2S^2\left(\frac{\beta-\alpha}{\beta+\alpha}\right)^2 - \frac{1}{\beta+\alpha}\right)^{\frac{1}{2}}, \tag{4.1}$$

where now

$$\alpha = I_0(\tilde{\gamma})/\tilde{\gamma}I_1(\gamma), \quad \beta = K_0(\tilde{\gamma})/\tilde{\gamma}I_0(\tilde{\gamma}). \tag{4.2a, b}$$

In the limiting case $\tilde{\gamma} \ll 1$,

$$\tilde{\sigma} = i\tilde{\gamma}(S \pm \tfrac{1}{2} \times 2^{\frac{1}{2}}), \tag{4.3}$$

which shows that these disturbances are stable. In the limiting case $\tilde{\gamma} \gg 1$,

$$\tilde{\sigma} = \pm(\tilde{\gamma}^2S^2 - \tfrac{1}{2}\tilde{\gamma})^{\frac{1}{2}}. \tag{4.4}$$

We may establish the stability criterion as follows. If $S > (2\tilde{\gamma})^{-\frac{1}{2}}$, the disturbance grows indefinitely. The larger the wavenumber, the easier it is to satisfy this criterion. Figure 3 is a graph of $\tilde{\sigma}_r$ *vs.* $\tilde{\gamma}$ [derived from (4.1)] for $S = 0{\cdot}4$, $0{\cdot}6$, $0{\cdot}8$ and $1{\cdot}0$. Note further that in the limit of large $\tilde{\gamma}$ the unstable waves do not propagate.

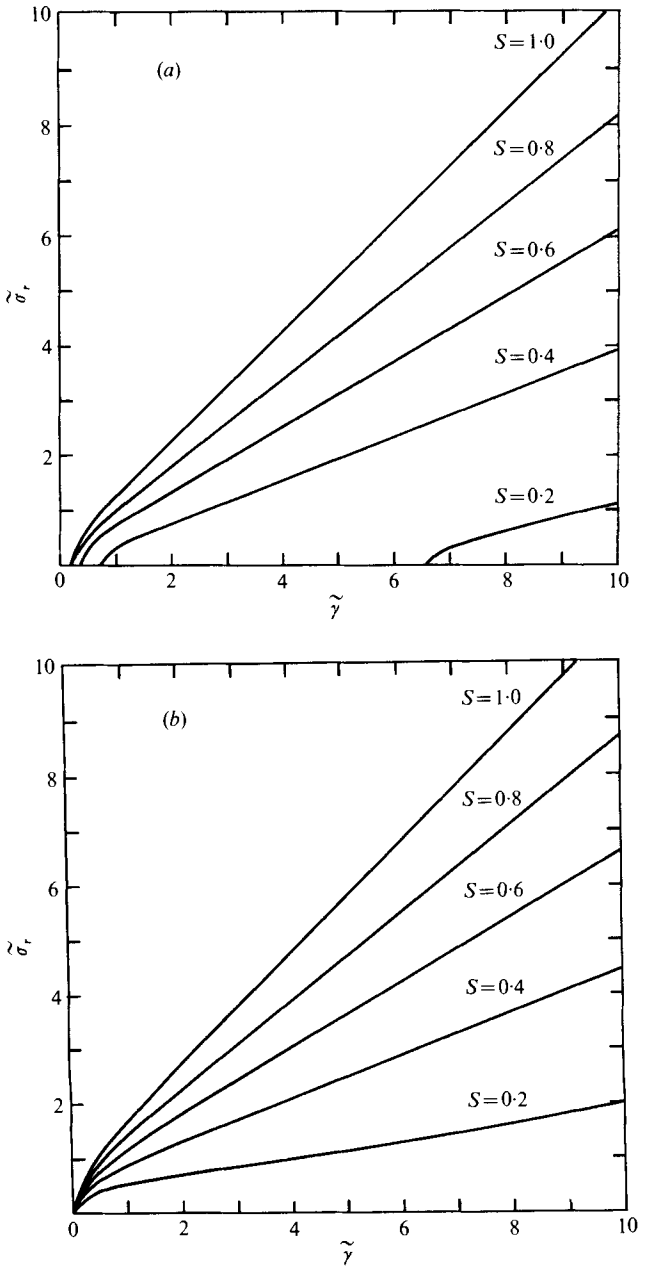


FIGURES 4(*a*, *b*). For legend see next page.

## 5. The full characteristic equation

Having examined the limits $S = 0$ and $m = 0$, respectively, we are in a better position to understand the behaviour of the full characteristic equation (2.20). Figure 4(*a*) displays $\tilde{\sigma}_r$ *vs.* $\tilde{\gamma}$ for $S = 0{\cdot}2$, $0{\cdot}4$, $0{\cdot}6$, $0{\cdot}8$ and $1{\cdot}0$ with $m = 1$. Comparison of figures 3 and 4(*a*) indicates that for a given $(S, \tilde{\gamma})$ the disturbance with the higher azimuthal wavenumber is more unstable. The reason for this is as follows. When

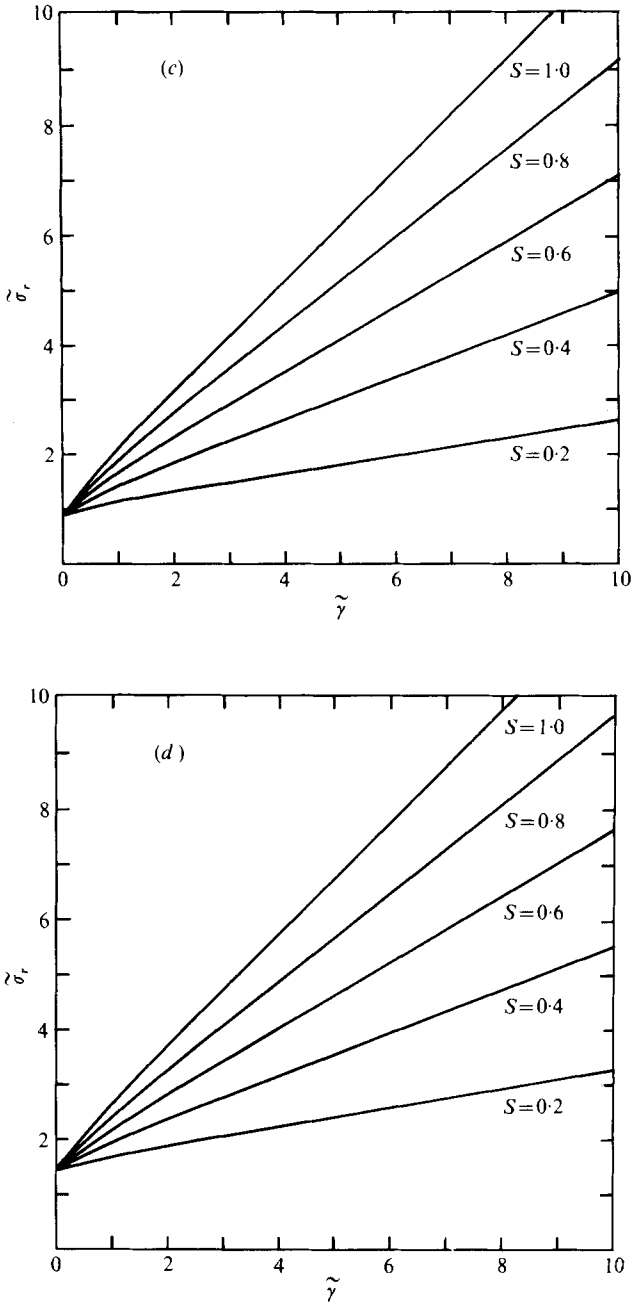


FIGURE 4. Non-dimensional growth rate $\tilde{\sigma}_r$ *vs.* the non-dimensional axial wavenumber $\tilde{\gamma}$ for $S = 0{\cdot}2$, $0{\cdot}4$, $0{\cdot}6$, $0{\cdot}8$ and $1{\cdot}0$ derived from (2.2). (*a*) $m = 1$, (*b*) $m = 2$, (*c*) $m = 3$ and (*d*) $m = 4$.

$m = 0$, the only instability mechanism is the radial shear in the mean vertical velocity. Having $m$ *and* $\tilde{\gamma}$ non-zero means that the wave can pick up energy from the radial shear in both the mean vertical and the mean azimuthal velocity. Notice that if $S \neq 0$ the modes $m = 1$ and 2 are unstable for sufficiently large $\tilde{\gamma}$. Hence the radial shear in the mean vertical velocity destabilizes these modes.

Figures 4(*b*)–(*d*) are the same as figure 4(*a*) except that $m = 2$, 3 and 4, respectively. Again, the growth rates are higher for larger $m$.

## 6. Radial angular momentum flux

Lilly (1969) argued that models which rely on an outward eddy diffusion to balance the inward advection of angular momentum are irrelevant to natural vortices. Using Hoecker's (1960, 1961) photogrammetric data, Lilly calculated the eddy radial angular momentum flux to be *inward*. He then hypothesized that this eddy flux is of second-order importance compared with the surface drag and hence neglected eddy fluxes in his model.

Using the solutions in § 2, we can compute the radial angular momentum flux due to the unstable waves:

$$F_i = (\overline{u_i v_i})_{r=R+\xi}, \quad i = 1, 2, \tag{6.1}$$

where the bar† denotes a wavelength average. It is easy to show that in region 1

$$F_1 = \overline{\left(\frac{\partial \phi_1}{\partial r}\right)\left(\frac{1}{R}\frac{\partial \phi_1}{\partial \theta}\right)} = 0. \tag{6.2}$$

The result in region 2 would also be zero if the term given in (2.8) had been omitted. In region 2,

$$F_2 = \overline{\left(\frac{\partial \phi_2}{\partial r}\right)\left(-\frac{\Gamma_0}{R^2}\xi + \frac{1}{R}\frac{\partial \phi_2}{\partial \theta}\right)} = -\frac{\Gamma_0}{R^2}\overline{\frac{\partial \phi_2}{\partial r}\xi}$$

and hence

$$F_2 = -\frac{\Gamma_0}{R^2}\frac{\sigma_r}{2}. \tag{6.3}$$

Thus for a growing disturbance ($\sigma_r > 0$), there is an associated inward radial angular momentum flux.

## 7. Discussion

The usual dilemma of this type of analysis is that the most unstable waves correspond to the smallest-scale disturbance. However, one resolves this problem to some extent by assuming that these small scales are quickly damped by a diffusion process. Analysis of flows with transition layers of finite thickness indicate that the most unstable waves have wavelengths of the same order as the transition-layer thickness. Indeed, the analysis for three concentric cylinders of Michalke & Timme (1967) and Busse (1968) yields this result.

On the basis of this knowledge, we offer the following tentative explanation for the vortex 'splitting' process. The 'vortex' as seen in Ward's (1972) experiment is actually a cylindrical vortext sheet of finite thickness. For a small swirl ratio the radius of the cylinder tends to be small, hence modes higher than two correspond to rather short azimuthal wavelengths which are probably damped. Modes $m = 1$ and 2 are stable. As the swirl ratio increases, the mean radius $R$ of the sheet increases and the destabilizing effect of the radial shear of the mean vertical velocity becomes more important. We conjecture that a most unstable wave will emerge whose azimuthal and vertical wavelengths are comparable to the finite vortex sheet thickness and

† Recall that $\overline{ab} = \frac{1}{2}(ab^* + a^*b)$, where $a^*$ is the complex conjugate of $a$.

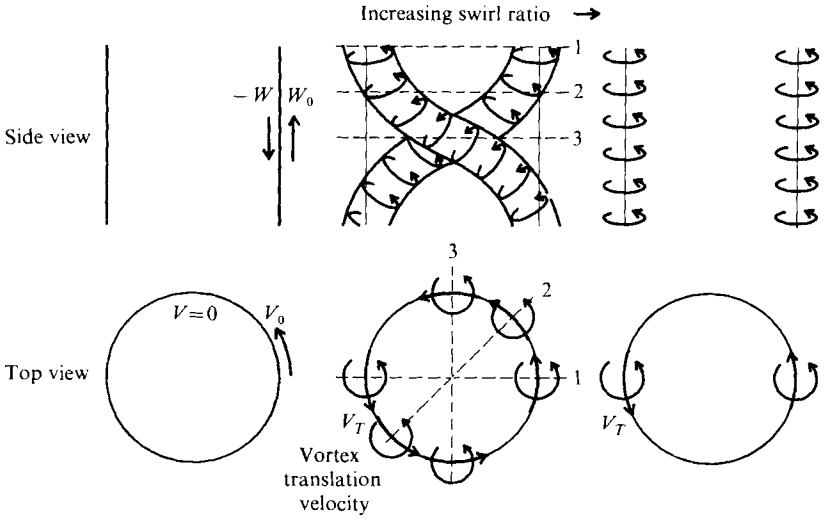


FIGURE 5. Schematic diagram of vortex 'splitting' process.

hence to each other. It is not unreasonable to expect that the wave $\tilde{\gamma} \sim m = 2$ may be that wave.

There is evidence (F. Leslie, private communication) that the vortex 'splitting' process has vertical structure. The first step in the vortex splitting process is a 'wrapping around' of two vortices as shown in figure 5. As the swirl ratio is increased, the two vortices 'straighten out' and separate. The description of the latter process appears to be beyond the reach of linear analysis.

## 8. Conclusions

We have resolved a certain inconsistency in Michalke & Timme's (1967) stability analysis of a cylindrical vortex sheet. It is found that azimuthal wavenumbers $m = 1$ and 2 are stable, whereas previously the stability of these modes was uncertain.

The cylindrical vortex sheet model is generalized to include a central downdraft surrounded by an updraft. We find that for a large enough swirl ratio modes $m = 0$, 1 and 2 are unstable (for axial wavenumbers $\tilde{\gamma} \neq 0$). We speculate on the implications of this for the multiple-vortex phenomenon.

There has been some controversy over the sign of the eddy radial flux of angular momentum in actual tornadoes. This analysis indicates that the growing waves are associated with an *inward* flux.

The National Center for Atmospheric Research is sponsored by the National Science Foundation.

## REFERENCES

BUSSE, F. H. 1968 Shear flow instabilities in rotating systems. *J. Fluid Mech.* **33**, 577.

DAVIES-JONES, R. P. 1976 Laboratory simulation of tornadoes. *Preprints Symp. Tornadoes: Assessments of Knowledge and Implications for Man, Texas Tech. Univ., Lubbock.*

FUJITA, T. T. 1971 Proposed mechanism for suction spots accompanied by tornadoes. *Preprints 7th Conf. Severe Local Storms, Am. Met. Soc.* p. 208.

HOECKER, W. H. 1960 Wind speed and air flow patterns in the Dallas tornado and some resultant implications. *Mon. Wea. Rev.* **88**, 167.

HOECKER, W. H. 1961 Three-dimensional pressure pattern of the Dallas tornado and some resultant implications. *Mon. Wea. Rev.* **89**, 533.

LILLY, D. K. 1969 Tornado dynamics. *N.C.A.R. Manuscript* no. 69–117.

MICHALKE, A. & TIMME, A. 1967 On the inviscid instability of certain two-dimensional vortex-type flows. *J. Fluid Mech.* **29**, 647.

WARD, N. B. 1972 The exploration of certain features of tornado dynamics using a laboratory model. *J. Atmos. Sci.* **29**, 1194.